Supporting Information for

The Iron-manganese bimetal -MOF with double mimic enzyme: DFT verification and colorimetric detection of Cr (VI)

Dehong Bai[1], Ziyu Xue[1], Shaohui Li[1], Ran Meng[1], Dongxia Zhang[1], Xibin Zhou[1,*]

1 Key Laboratory of Resource Environment and Sustainable Development of Oasis, College of Geography and Environment Science, Northwest Normal University, Lanzhou 730070, China

E-mail address of Corresponding author:
zhouxb@nwnu.edu.cn (Xibin Zhou).

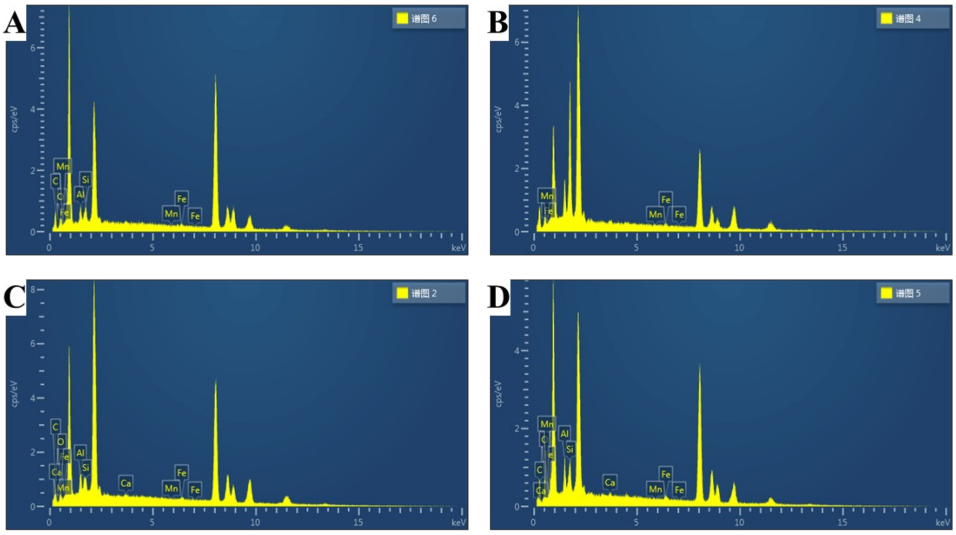

Fig. S1 EDX pattern of (A) Fe_3Mn_1-MOF, (B) Fe_2Mn_1-MOF, (C) Fe_1Mn_1-MOF, (F) Fe_1Mn_2-MOF.

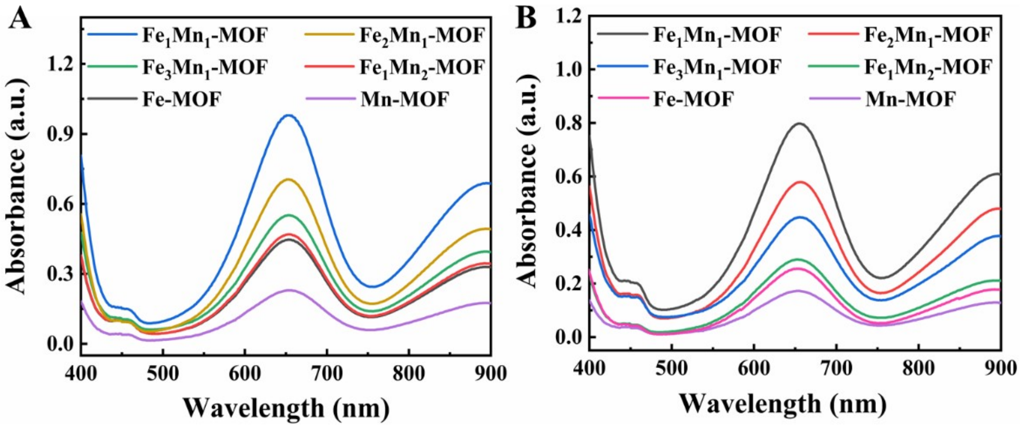

Fig. S2 UV–vis absorption spectra of TMB catalyzed by different composite in system (A) TMB + H_2O_2 + Fe_xMn_y-MOF; (B) TMB +Fe_xMn_y-MOF.

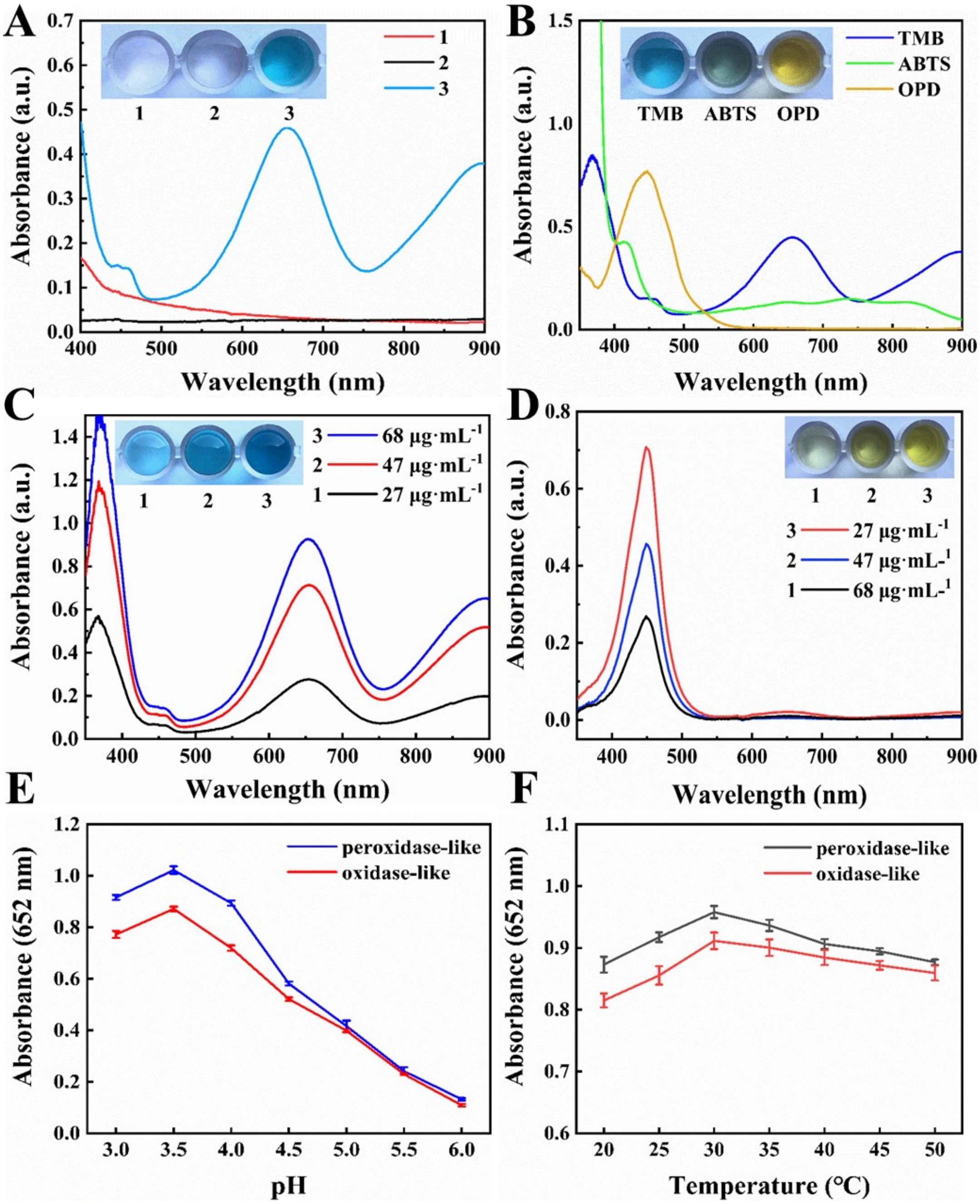

Fig. S3 (A) UV-vis absorption spectra and color changes of TMB in different reaction systems: (1) Fe_1Mn_1-MOF, (2) TMB, (3) TMB + Fe_1Mn_1-MOF; (B) The oxidation of various substrates catalyzed by Fe_1Mn_1-MOF. (C) The UV-vis spectra of TMB catalyzed by different concentrations of Fe_1Mn_1-MOF; (D) UV-vis spectra of different concentrations of Fe_1Mn_1-MOF after adding sulfuric acid. The effects of (E) pH and (F) temperature on the mimic enzyme activity.

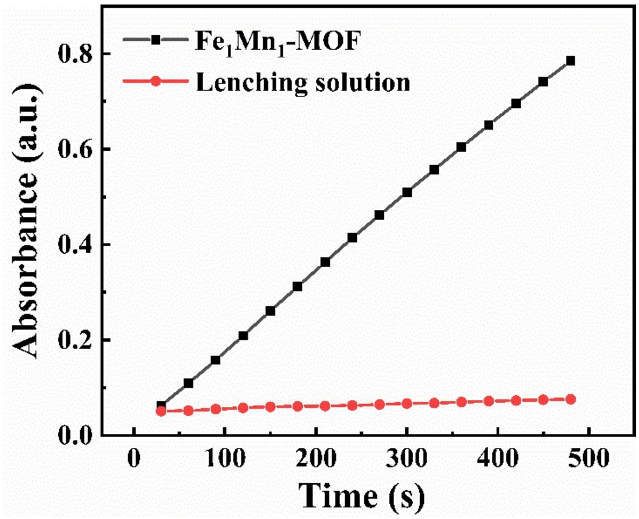

Fig. S4 Absorbance at 652 nm of the TMBox system as a function of time in two solutions (black line: Fe_1Mn_1-MOF, red line: leaching solution).

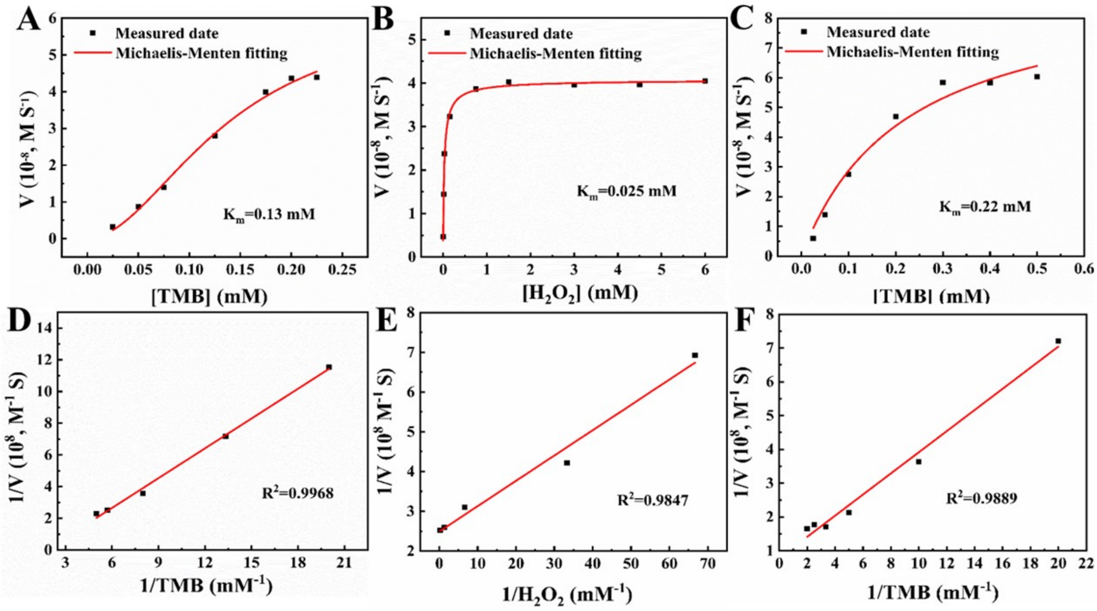

Fig. S5 Steady-state kinetic analyses using the Michaelis–Menten curves (A, B and C) and the Lineweaver–Burk plots (D, E and F) for Fe_1Mn_1-MOF. (A and D) the TMB concentration was altered, (B and E) the H_2O_2 concentration was altered, and (C and F) the concentration of TMB was altered without H_2O_2.

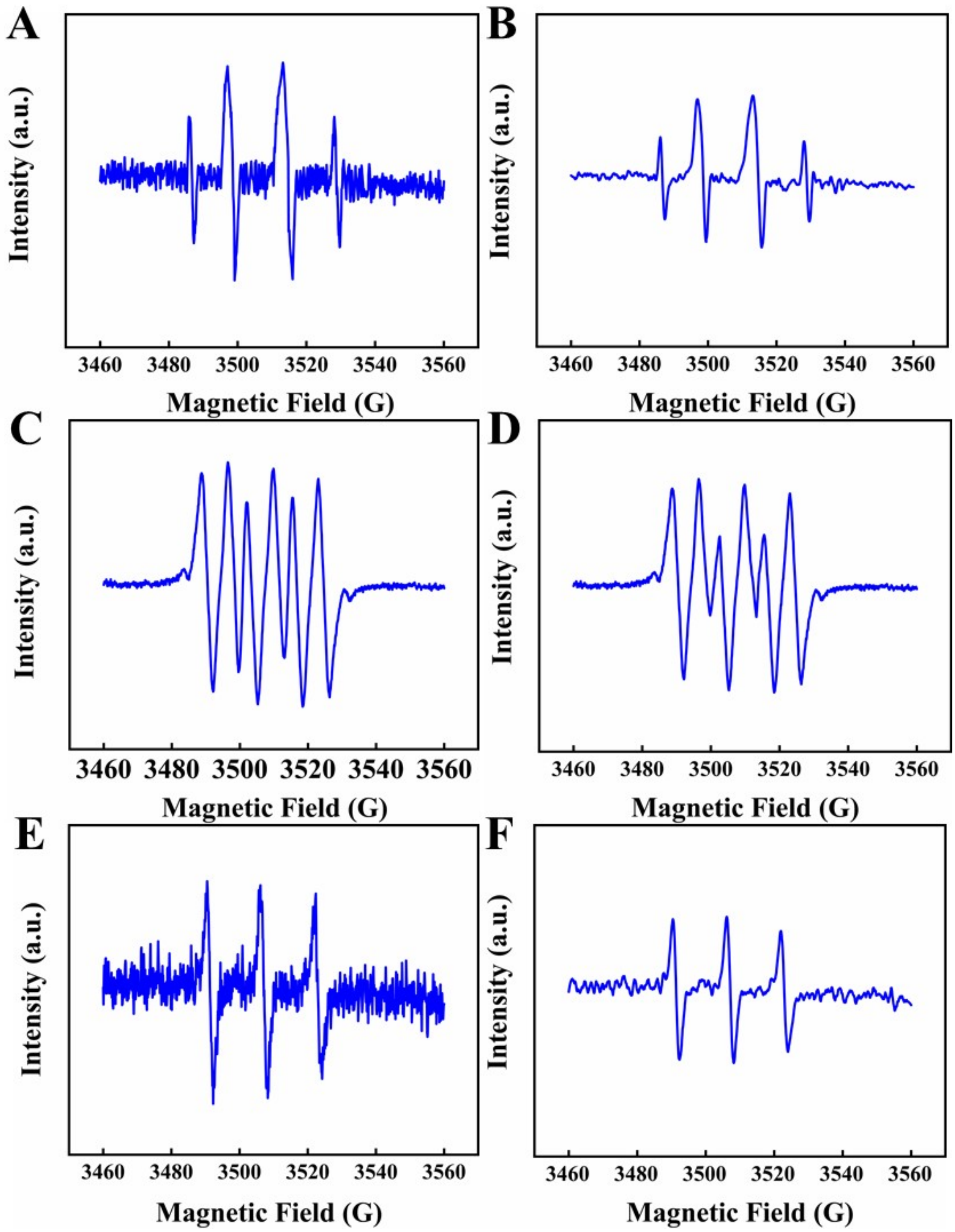

Fig. S6 ESR spectra of Fe_1Mn_1-MOF+H_2O_2 in (A) H_2O for DMPO-•OH, (C) H_2O for DMPO-•O_2^-, and (E) H_2O for TEMP-$^1O_2$. ESR spectra of Fe_1Mn_1-MOF composite without H_2O_2 for DMPO-•OH, DMPO-•O_2^-, and TEMP-$^1O_2$ are shown in B, D, and F, respectively.

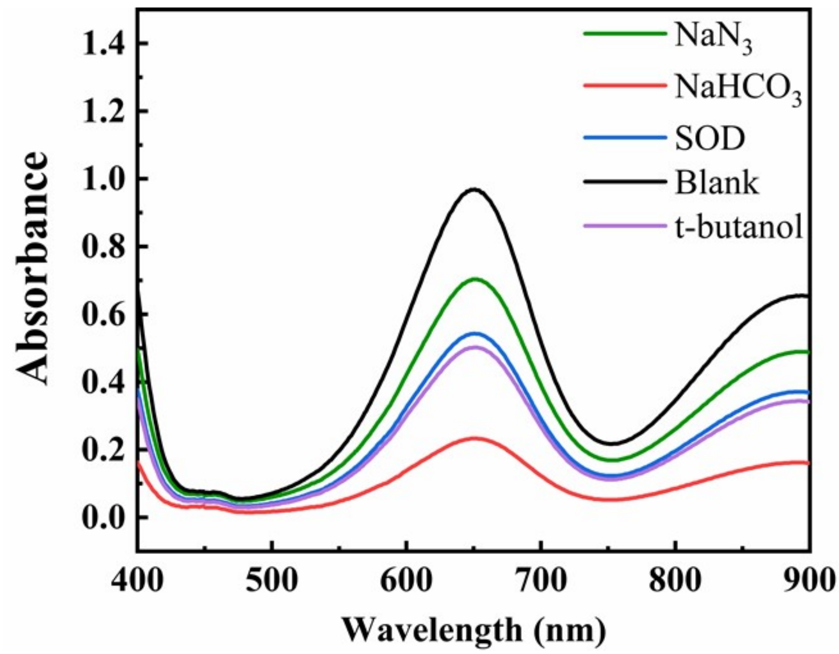

Fig. S7 UV-vis spectra of different reactive oxygen species scavengers added to the system.

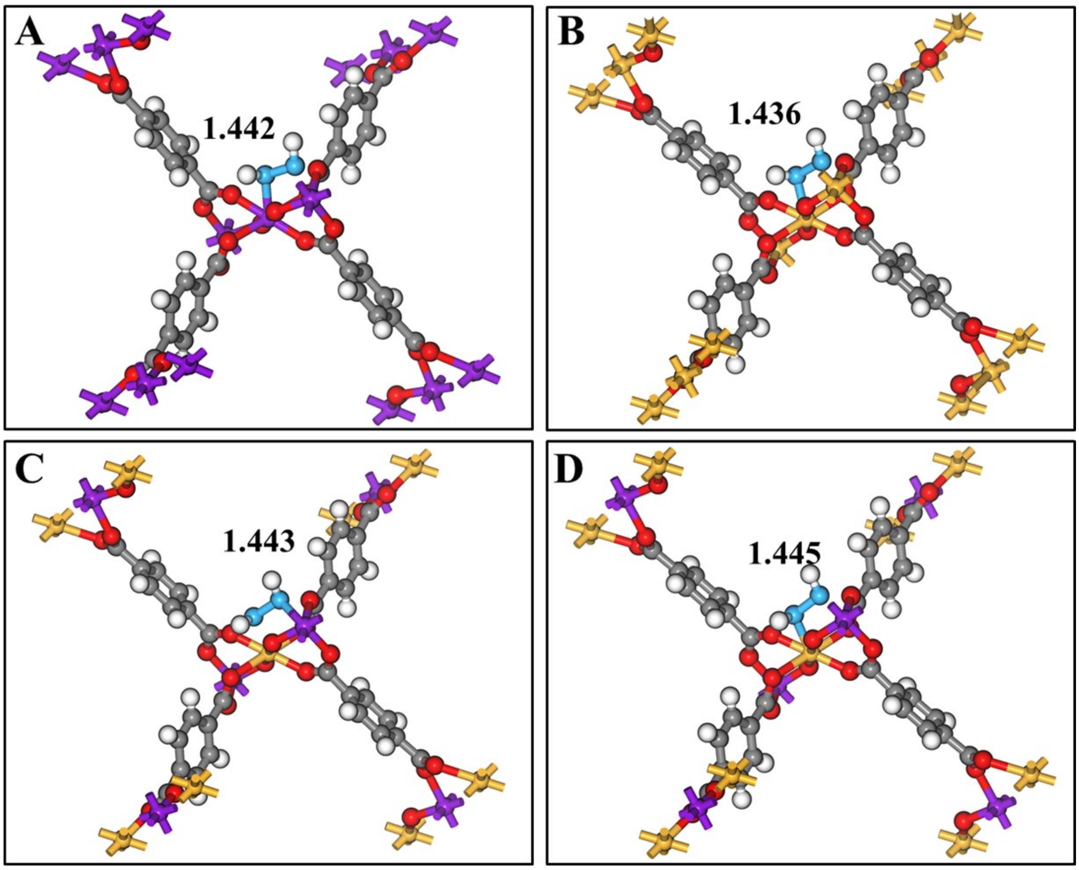

Fig. S8 Configurations of adsorption of H_2O_2 on different models: (A) Mn-MOF; (B) Fe-MOF; (C) Fe_1-Mn_1-MOF (Mn*); (D) Fe_1-Mn_1-MOF (Fe*).

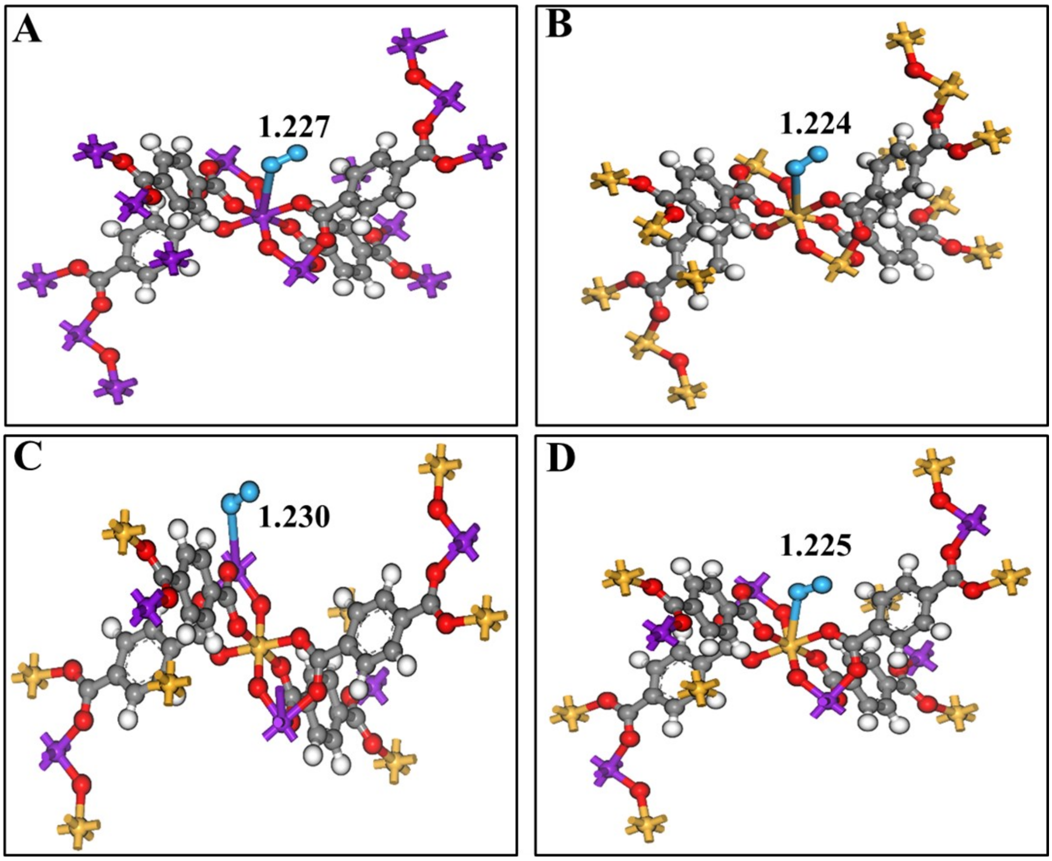

Fig. S9 Configurations of adsorption of O_2 on different models: (A) Mn-MOF; (B) Fe-MOF; (C) Fe_1-Mn_1-MOF (Mn*); (D) Fe_1-Mn_1-MOF (Fe*).

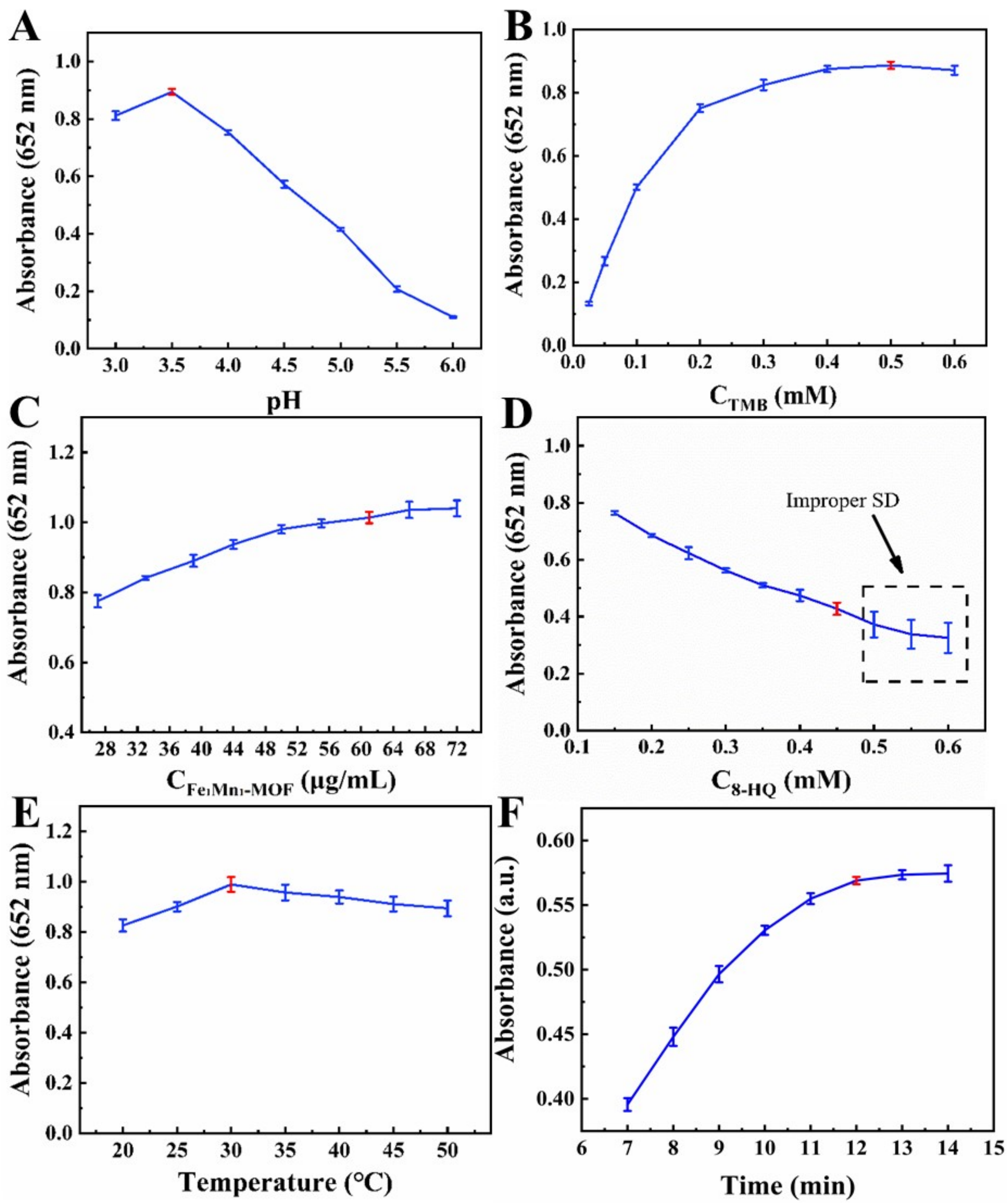

Fig. S10 The influences of buffer solution pH (A); concentration of TMB (B); concentration of Fe_1-Mn_1-MOF (C);concentration of 8-HQ (D); Temperature (E); responsive time (F) on the system (Fe_1-Mn_1-MOF: 60 μg/mL, TMB: 0.5 mM, 8-HQ: 0.45 mM, Cr (VI): 3000 nM).

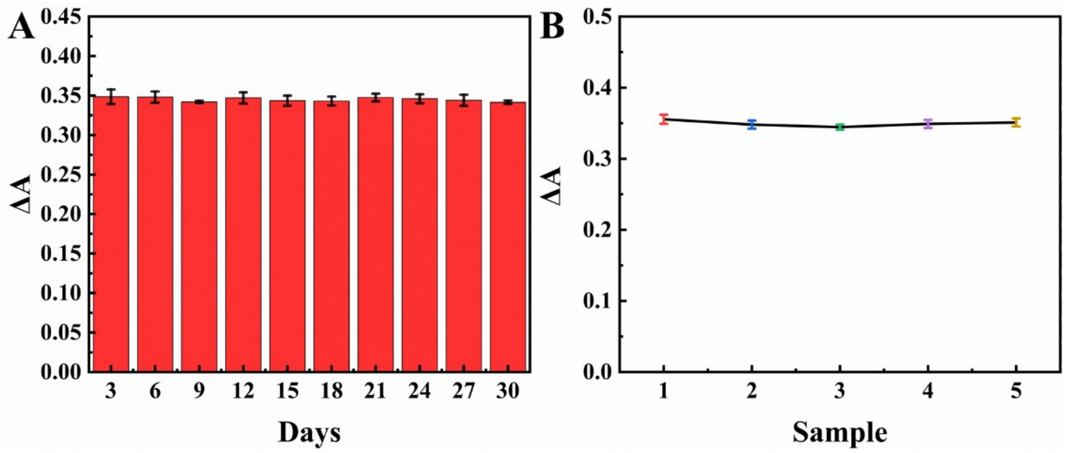

Fig. S11 (A) Variation of catalytic activity of the Fe_1Mn_1-MOFs with time through 30 days; (B) The Absorbance difference (ΔA) at 652 nm of five sample solutions with the same Cr(VI) concentration.

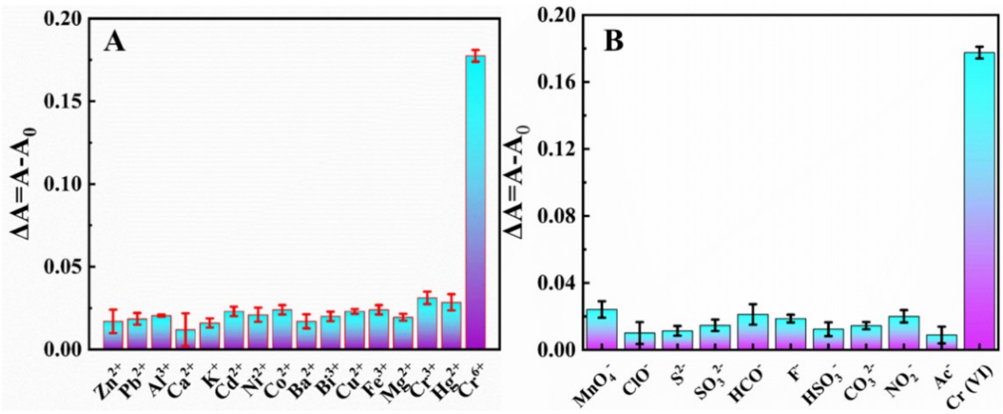

Fig. S12 Anti-interference experiment for colorimetric detection of Cr (VI). (A) cation, (B) anion.

Table. S1 Compared the apparent Michaelis-Menten constant (K_m) and maximum reaction rate (V_{max}) between the Fe_1Mn_1-MOF and other nanozyme.

Catalyst	Substrate	K_m (mM)	V_{max} (×10-8 , M/s)	Ref
HRP	TMB	0.434	10.00	[1]
	H_2O_2	3.70	0.871	
Glycine-MIL53(Fe)	TMB	0.11	2.28	[2]
	H_2O_2	0.10	2.25	
MOF(Co/2Fe)	TMB	0.25	3.78	[3]
	H_2O_2	4.22	4.91	
Fe_2Ni-MOF	TMB	0.557	3.039	[4]
	H_2O_2	0.134	1.35	
Fe_1Mn_1-MOF	TMB	0.13	6.34	This work
	H_2O_2	0.025	3.99	

Table. S2 The Michaelis-Menten constant (K_m) and maximum reaction rate (V_{max}) of the Fe_1Mn_1-MOF with TMB as the substrate.

Catalyst	Substrate	K_m (mM)	V_{max} (×10-8 ,	Ref
PCN-224-Mn	TMB	0.243	13.725	[5]
MOF(Co/2Fe)	TMB	0.20	0.39	[3]
Co/Mn-MOFs	TMB	0.27	16.4	[6]
Fe_1Mn_1-MOF	TMB	0.22	9.23	This work

Table. S3 It was compared with other methods for detecting Cr (VI) in water samples.

Material	Method	Linear range	LOD	Ref
MOF-199 (Cu)	Colorimetric	100-30000 nM	20 nM	[7]
GO	Colorimetric	70-430 nM	6 nM	[8]
Zn (II)-MOF	Fluorescence	/	6.91 μM	[9]
Co-CDs	Fluorescence	5-125μM	1.17 μM	[10]
BSA-Au NP	Colorimetric	0.5-5- μM	280 nM	[11]
Siloxane-thiourea	Fluorescence	0-20 μM	63 nM	[12]
SnS/Bi_2MoO_6	Electrochemical	0.5-310 μM	0.122 μM	[13]
PANI/Hep/MTA/ MGCE	Electrochemical	10^{-4}-10^{-7} ppm	0.87 μM	[14]
Fe_1Mn_1-MOF	Colorimetric	80-3500 nM	51 nM	This work

References:

[1] D. Bai, Z. Xue, P. Guo, M. Qiu, X. Lei, Y. Li, C. Ma, D. Zhang, X. Zhou, Ultrasensitive colorimetric detection of Hg2+ based on Glutathione-modified Au nanoflowers, Microchemical Journal (2022).

[2] W. Dong, L. Yang, Y. Huang, Glycine post-synthetic modification of MIL-53(Fe) metal-organic framework with enhanced and stable peroxidase-like activity for sensitive glucose biosensing, Talanta 167 (2017) 359-366.

[3] H. Yang, R. Yang, P. Zhang, Y. Qin, T. Chen, F. Ye, A bimetallic (Co/2Fe) metal-organic framework with oxidase and peroxidase mimicking activity for colorimetric detection of hydrogen peroxide, Microchimica Acta 184(12) (2017) 4629-4635.

[4] Z. Mu, S. Wu, J. Guo, M. Zhao, Y. Wang, Dual Mechanism Enhanced Peroxidase-like Activity of Iron–Nickel Bimetal–Organic Framework Nanozyme and Its Application for Biosensing, ACS Sustainable Chemistry & Engineering 10(9) (2022) 2984-2993.

[5] X. Lai, Y. Shen, S. Gao, Y. Chen, Y. Cui, D. Ning, X. Ji, Z. Liu, L. Wang, The Mn-modified porphyrin metal-organic framework with enhanced oxidase-like activity for sensitively colorimetric detection of glutathione, Biosens Bioelectron 213 (2022) 114446.

[6] X. Qi, Tian, H., Dang, X., Fan, Y., Zhang, Y., Zhao, H., Anal. Methods. (2019).

[7] W. Shi, M. He, W. Li, X. Wei, B. Bui, M. Chen, W. Chen, Cu-Based Metal–Organic Framework Nanoparticles for Sensing Cr(VI) Ions, ACS Applied Nano Materials 4(1) (2021) 802-810.

[8] N.N. Nghia, B.T. Huy, Y.I. Lee, Colorimetric detection of chromium(VI) using graphene oxide nanoparticles acting as a peroxidase mimetic catalyst and 8-hydroxyquinoline as an inhibitor, Mikrochim Acta 186(1) (2018) 36.

[9] H. Jin, J. Xu, L. Zhang, B. Ma, X. Shi, Y. Fan, L. Wang, Multi-responsive luminescent sensor based on Zn (II) metal-organic framework for selective sensing of Cr(III), Cr(VI) ions and p-nitrotolune, Journal of Solid State Chemistry 268 (2018) 168-174.

[10] H.Y. Zhang, Y. Wang, S. Xiao, H. Wang, J.H. Wang, L. Feng, Rapid detection of Cr(VI) ions based on cobalt(II)-doped carbon dots, Biosens Bioelectron 87 (2017) 46-52.

[11] J.F. Guo, D.Q. Huo, M. Yang, C.J. Hou, J.J. Li, H.B. Fa, H.B. Luo, P. Yang, Colorimetric detection of Cr (VI) based on the leaching of gold nanoparticles using a paper-based sensor, Talanta 161 (2016) 819-825.

[12] X. Wang, Z. Gou, Y. Zuo, Thioureas Bridged Polysiloxanes for Ultrafast Detection of Cr6+ and Applications, Macromolecular Chemistry and Physics 222(13) (2021).

[13] Y. Wang, Y. Ma, Q. Zhao, L. Hou, Z. Han, Polyoxometalate-based crystalline catalytic materials for efficient electrochemical detection of Cr(VI), Sensors and Actuators B: Chemical 305 (2020) 127469.

[14] D. Fang, T. Xu, L. Fang, H. Chen, Y. Huang, H. Zhang, Z. Miao, C. Mao, B. Chi, H. Xu, A blood compatible, high-efficient sensor for detection of Cr(VI) in whole blood, Sensors and Actuators B: Chemical 329 (2021).